Letter

Phonon modulated hopping polarons: *x*-representation technique

Nikolay V. Prokof'ev[1] and Boris V. Svistunov[1,2]
[1]*Department of Physics, University of Massachusetts, Amherst, Massachusetts 01003, USA*
[2]*Wilczek Quantum Center, School of Physics and Astronomy, and T. D. Lee Institute, Shanghai Jiao Tong University, Shanghai 200240, China*

(Received 5 May 2022; accepted 14 July 2022; published 27 July 2022)

We report a breakthrough development allowing one to solve a broad class of polaron problems with highly nonlinear electron-phonon coupling that were considered unsolvable without uncontrolled simplifications in the past using a Monte Carlo technique formulated in the coordinate representation for both the particle and the atomic displacements. The only condition is the sign positivity of the hopping amplitude. The technique dramatically simplifies (with the corresponding efficiency gains) for models with dispersionless phonons. Our study sheds important light on the nature and universality of the most striking qualitative and quantitative effects demonstrated by the "standard" (Peierls/Su-Schrieffer-Heeger) model based on the linearized displacement-modulated hopping.

DOI: 10.1103/PhysRevB.106.L041117

Introduction. The effect of phonons on particle motion in an elastic lattice has been of interest for a long time [1–14]. Recent progress is motivated by results for the Peierls/Su-Schrieffer-Heeger (PSSH) model with linear dependence of tunneling on atomic displacements [5,6,9,10]; see an illustration in Fig. 1. PSSH polarons differ dramatically from their counterparts based on the density-displacement coupling. One distinction—important in the context of the bipolaron mechanism of superconductivity—is the absence of sharp self-trapping crossover and steep increase of the effective mass in the adiabatic regime when the phonon frequency Ω is much smaller than the particle bandwidth. Another feature of PSSH polarons is the shift of the ground-state momentum to finite values at strong coupling [5,6,9,10].

The general form of the phonon modulated hopping term between lattice sites j and i is

$$-t_{ij}(\{x_s\})a_j^\dagger a_i, \tag{1}$$

where $a_j^\dagger$ is the particle creation operator, and t_{ij} is the hopping amplitude depending on a set of atomic displacements x_s. To define the class of models solvable by Monte Carlo (MC) methods, consider Eq. (1) in the x representation when atomic displacements and, thus, hopping amplitudes are real numbers. In many cases, the textbook double-well potential problem being one of them, $t_{ij}(\{x_s\})$ is sign definite. However, when $t_{ij}(\{x_s\})$ is approximated by a linear function of $\{x_s\}$, as is typically done for PSSH-type models, the sign-definiteness property is violated for large displacements. This raises two questions: what is known about PSSH polarons with highly nonlinear coupling to phonons, and is sign-changing t_{ij} a key ingredient behind the special properties of "linearized" PSSH polarons?

For decades, it was believed that numerically exact studies were possible only for models with linear coupling to phonons, leading to questionable simplifications of physics at strong coupling and displacement. In our approach, the linearity of the coupling plays no role, and the only necessary and sufficient condition is that the particle's hopping amplitude be sign positive (or sign definite on bipartite lattices). In this Letter, we provide first-principle numeric evidence that unusual properties of linearized PSSH polarons are absent in a nonlinear model with sign-positive t_{ij}. Our approach is based on the observation that sign-definite t_{ij} leads to a sign-positive path-integral formulation in the x representation. For dispersionless phonons a substantial part of the path integral is performed analytically, resulting in a simple and efficient diagrammatic-type ground-state MC scheme.

Model Hamiltonian. Since unusual properties of PSSH polarons are captured by the linearized one-dimensional model with dispersionless phonons [5,6,9,10], we consider here its positive-t_{ij} extension:

$$H = H_1 + H_2 = -\sum_{\langle ij\rangle} t(x_i, x_j)a_j^\dagger a_i + \Omega\sum_i b_i^\dagger b_i, \tag{2}$$

where b_i is the phonon annihilation operator on site i, $x_i = b_i^\dagger + b_i$ is the dimensionless harmonic oscillator coordinate, and $j = i \pm 1$ goes over all nearest-neighbor sites. We count energy from the ground state of the phonon field. A simple physical model for t_{ij} dependence on the relative displacement, ΔR_{ij}, is formulated as

$$t(x_i, x_j) = t_0 e^{-S(a\mp\Delta R_{ij})^2/a^2}, \quad \Delta R_{ij} = u(x_i - x_j), \tag{3}$$

with $\mp$ being the sign for hopping in the positive/negative axis direction (see Fig. 1). Here $S \gg 1$ is the tunneling action in the rigid lattice with lattice spacing a, and $u = 1/\sqrt{2M\Omega}$ is the zero-point motion amplitude of an atom of mass M. An equivalent reparametrization would be

$$t(x_i, x_j) \equiv t e^{\pm g(x_i - x_j) - \epsilon(x_i - x_j)^2}, \tag{4}$$

with $t = t_0 e^{-S}$, $g = 2S(u/a)$, and $\epsilon = S(u/a)^2 = g^2/4S$. The linearized model corresponds to $t(x_i, x_j) \approx t \pm gt(x_i - x_j)$. In

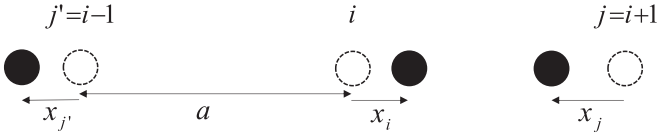

FIG. 1. Tunneling amplitude depends on the distance between the atoms and is enhanced (suppressed) when they move closer to (away from) each other. This leads to the sign-alternating dependence on x_i when the particle moves in the positive *vs* the negative lattice direction [see Eqs. (3) and (4)].

what follows, we set t as the unit of energy and treat ϵ and g as independent parameters to get a broader perspective on the model properties.

To begin with, the $\epsilon = 0$ case is pathological. Indeed, one gains a divergent amount of energy from particle delocalization between just two neighboring sites shifted relative to each other by $|x| = |x_i - x_{i+1}| \to \infty$. Finite ϵ provides a regularization, and the $\epsilon \to 0$ limit can be understood by considering the minimum of the sum of the oscillator potential energy and the particle kinetic energy gain as a function x:

$$E(x) = \Omega x^2/4 - t \exp\{gx - \epsilon x^2\}. \tag{5}$$

As long as ϵ is very small (e.g., because of a small u/a ratio), the system undergoes a drastic crossover at small $g \approx g_\epsilon \sim \sqrt{\epsilon}$ from a perturbative state to a self-trapped one. To the leading approximation, the self-trapped state corresponds to the particle delocalized between the two nearest sites undergoing a large displacement, $x \gg 1$; quantum fluctuations of x and tunneling of the self-trapped state yield small corrections to the ground-state energy $E_G \approx \min_x E(x)$. In accordance with Eq. (5), see also Fig. 2, the self-trapped state with $E_G \propto -te^{g^2/4\epsilon}$ exists at $g > g_\epsilon$, while at $g < g_\epsilon$ a perturbative treatment of the particle-phonon coupling is justified: $E_G \approx -t - g^2t^2/\Omega$,

Qualitatively, a sharp self-trapping crossover at $g \ll 1$ is generic for any tight-binding model characterized by pronounced exponential dependence of hopping on atomic coordinates and some physical mechanism (parametrized by a small parameter) limiting $t(x_i, x_j)$ for large displacements—an analog of our ϵ. This consideration rules out prospects for having light polarons in model (2) and its analogs at strong coupling when linear coupling is exponentiated,

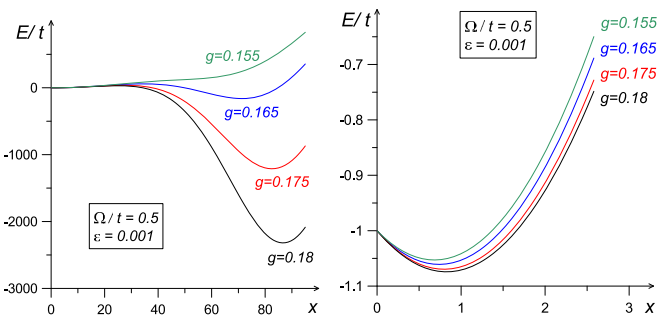

FIG. 2. Energy landscape (5) for small $\epsilon = 0.001$ at large and small values of x. A deep minimum ($|E_{\min}| \gg \Omega, t$) at $x \gg 1$ corresponds to the self-trapped state. In the absence of such a minimum the polaron state is perturbative.

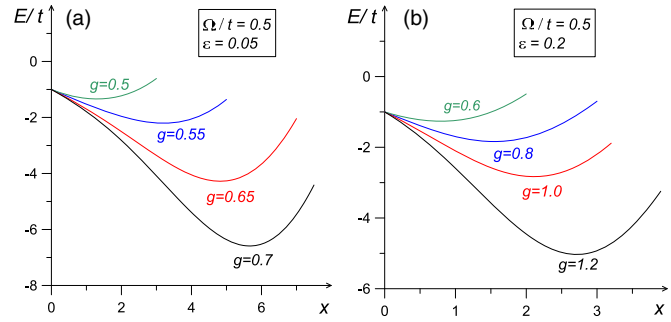

FIG. 3. Energy landscape (5) at $\epsilon = 0.05$ (a) and $\epsilon = 0.2$ (b). The absence of a deep ($|E_{\min}| \gg \Omega, t$) minimum at $x \gg 1$ indicates a smooth crossover of polaron properties from weak to strong coupling.

$t(1 - gx) \to te^{-gx}$, and the exponent is allowed to have large values. Only in the perturbative regime (i.e., at $g < g_\epsilon$) do the exponential and linearized models produce similar results.

When ϵ is increased, the situation changes dramatically as illustrated in Fig. 3. Now the energy minimum is unique for any value of g. At $\epsilon = 0.05$, a smooth crossover to the exponential energy-gain regime still takes place at moderate values of g. At $\epsilon = 0.2$, the regime of strong coupling $g \gtrsim 1$ considered in the previous work can be reached more easily, see Fig. 3(b), and the most intriguing question that can only be answered by a full quantum mechanical solution is whether the ground-state momentum in this case remains zero or shifts to finite values as in the linearized model.

x representation. Within the coordinate representation for both the particle and the phonons one can formulate a sign-positive MC approach to a broad class of polaron problems with arbitrary particle-phonon interactions, of the density-displacement or/and hopping-displacement type, provided the latter are sign positive. This is readily seen with the standard path-integral representation, where the only condition for the scheme to be sign positive is the requirement $t_{ij}(\{x_s\}) \gtrsim 0$.

Conventional path-integral treatment of phonons in the x representation would force one to deal with the $(d+1)$-dimensional configuration space, with the finite system size L, finite inverse temperature β, and finite imaginary-time step $\Delta\tau$. Correspondingly, the MC results would need to be extrapolated towards the $L, \beta \to \infty$ and $\Delta\tau \to 0$ limits. However, the harmonic nature of lattice vibrations allows one to partially integrate phonon x paths analytically. There are two ways of achieving this goal. The first one is particularly suited for dispersionless phonons considered in this work. An alternative approach utilizes the sign-positive diagrammatic expansion discussed in the Conclusions and Outlook section.

The Gaussian form of the free phonon propagators in the x representation allows one to perform semianalytic integration over all x variables except for those whose values parametrize the magnitudes of particle hopping amplitudes and thus have to be sampled along with the particle worldlines. This naturally leads to the thermodynamic ($L \to \infty$) formulation. In addition (and along similar lines), the Gaussian form of the ground-state wave function allows one to formulate an explicit ground-state technique for the imaginary-time polaron

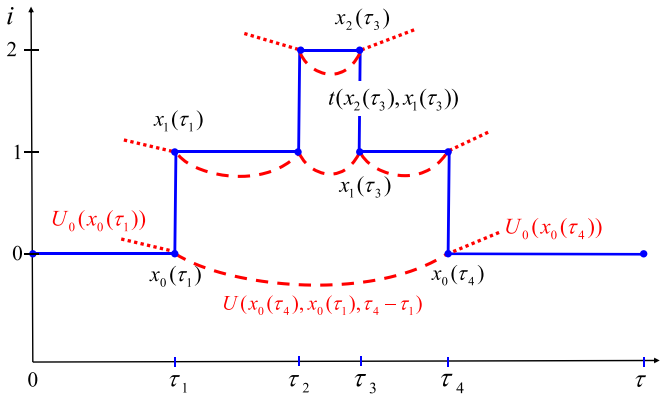

FIG. 4. Typical x-representation diagram for the Green's function $\mathcal{G}(\tau, r)$ of the model (2). The blue solid line is the particle worldline with kinks—the vertical segments—representing the hopping amplitudes t. Dashed and dotted red lines represent the phonon propagators U and U_0, respectively. Propagators U_0 behave as τ-independent vertices because the phonon ground-state energy is set to zero.

Green's function in the site representation:

$$\mathcal{G}(\tau, r) = \langle a_r(\tau) a_0^\dagger(0) \rangle. \tag{6}$$

Here τ is the imaginary time, r is the (discrete) distance from the origin, and $\langle \cdots \rangle$ stands for averaging over the ground state of the system.

In general, the necessity of performing macroscopic Gaussian integration when making local updates changing a couple of variables might bring little advantage compared to sampling full worldline configurations by local updates. However, the gain is dramatic in the case of dispersionless (i.e., spatially local) phonon modes. Here the paths for phonon modes on different sites are *disconnected*—and thus do not need to be sampled—as long as their x variables are not associated with the hopping events on the particle's worldline. Projection to the ground state of harmonic oscillators involves special (mixed representation) phonon x propagators,

$$U_0(x, \tau) = \langle G | e^{-\tau H_2} | x \rangle = \langle x | e^{-\tau H_2} | G \rangle,$$

connecting the phonon mode ground states $\langle G|$ and $|G\rangle$ (at the left and the right ends of the path, respectively) to the corresponding closest in time hopping events controlled by the given mode. The special propagators $U_0(x, \tau)$ are related to generic phonon x propagators,

$$U(y, x, \tau) = \langle y | e^{-\tau H_2} | x \rangle,$$

by the obvious relation $U_0(y, \tau) = \int U(y, x, \tau)\, \psi_0(x)\, dx$, where $\psi_0(x)$ is the ground-state wave function of the phonon mode in the x representation. Thanks to our choice of the phonon ground-state energy, U_0 propagators are τ independent as follows from

$$U_0(y) = \langle y | e^{-\tau H_2} | G \rangle \equiv \langle y | G \rangle = \psi_0(y) = \frac{e^{-y^2/4}}{(2\pi)^{1/4}}. \tag{7}$$

A typical "diagram" for $\mathcal{G}(\tau, r)$ is shown in Fig. 4. The product of all phonon propagators and hopping amplitudes in the graph with n hopping transitions constitutes the configuration weight W_n. An explicit expression for the propagator $U(y, x, \tau)$ is given by

$$U(y, x, \tau) = \frac{e^{(1/2)\Omega\tau - Q(y,x,\tau)}}{\sqrt{4\pi \sinh(\Omega\tau)}},$$

$$Q(y, x, \tau) = \frac{\cosh(\Omega\tau)(x^2 + y^2) - 2xy}{4 \sinh(\Omega\tau)}. \tag{8}$$

As long as all the phonon modes are local, adding the density-displacement (e.g., Holstein) couplings on top of the hopping-displacement ones comes at little computational cost. The effect of standard linear and quadratic x variables in density-displacement interactions is readily accounted for by an analytic modification of Gaussian x propagators for every segment of the particle worldline between two adjacent hopping events (linear and quadratic density-displacement couplings lead to a modified shifted harmonic oscillator Hamiltonian); the cost for treating generic density-displacement interactions is also moderate-numeric tabulation of the x propagator. If the density-displacement coupling is to the very same modes that control the value of the hopping amplitude, then we deal with exactly the same diagrams as in Fig. 4, but now with modified x propagators. If the density-displacement coupling is to separate phonon modes, one needs to introduce propagators for those modes and sample the corresponding x variables specified at all sites connected by the particle hopping transitions.

Monte Carlo scheme. The sign-positive diagrammatic-type expansion for $G(\tau, r)$ in powers of hopping transitions leads to a simple and efficient diagrammatic Monte Carlo [15,16] simulation protocol. Our scheme is based on updates that change (i) the variable τ [the τ update], (ii) the variable $x_{r_k}(\tau_k)$ or $x_{r_k}(\tau_{k-1})$ [the x update], and (iii) the expansion order, n, by ± 1 [the $(n \pm 1)$ updates].

(i) In the τ update, the new value $\tau' > \tau_n$ is proposed from the exponential probability distribution $P(\tau') = -e^{\mu(\tau' - \tau_n)}/\mu$. Here τ_n is the time moment of the nth (i.e., the last one in the time domain) kink and $\mu < 0$ is an auxiliary parameter introduced for controlling the Green's function statistics in the time domain. This update is always accepted.

(ii) In the x update, we select at random one of the hopping transitions and propose to update the oscillator coordinate at one of the two sites involved. This update changes the product of all phonon propagators depending on this coordinate times the value of the hopping amplitude. Since all the functions involved are Gaussian functions of the updated oscillator coordinate, the x update is rendered rejection free by proposing the new coordinate, x', from the Gaussian distribution

$$P(x') = (2\pi\sigma^2)^{-1/2} \exp[-(x' - z)^2/2\sigma^2],$$

with the shift z and dispersion σ depending on other relevant graph variables.

(iii) In the $(n + 1)$ update, called with probability p_+, we propose to insert a kink between the sites $R = r_n(\tau_n)$ and $R' = r_{n+1}(\tau_{n+1})$. The time τ_{n+1} is selected from the uniform distribution on the interval (τ_n, τ) and $R' = R \pm 1$ is selected at random. The new oscillator variables $x_R(\tau_{n+1}) = y$ and $x_{R'}(\tau_{n+1}) = z$ are proposed from the Gaussian distribution

$$P(x, y) \propto e^{-(y^2+z^2)/2 \pm g(y-z) - \epsilon(y-z)^2}.$$

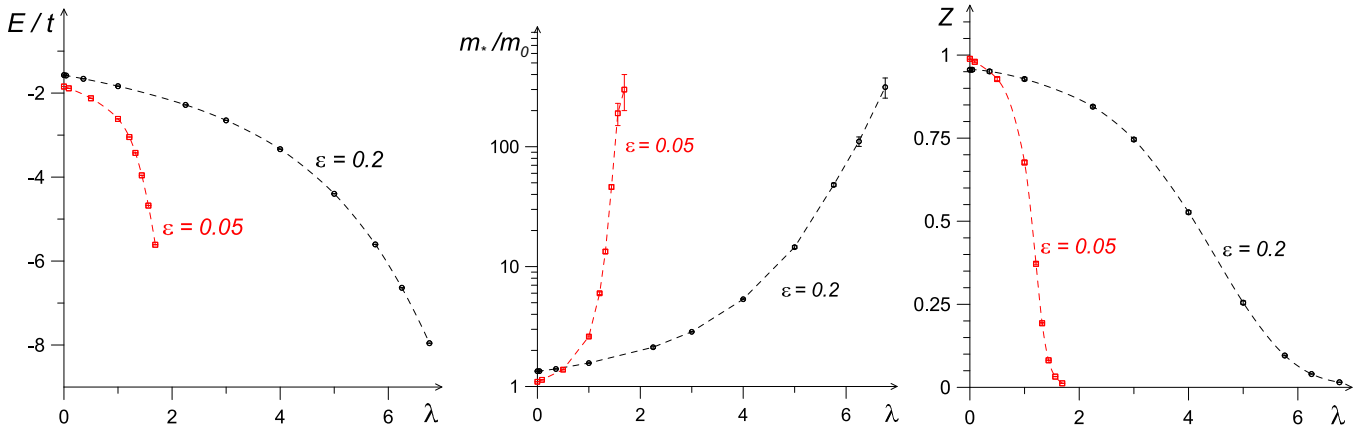

FIG. 5. Energies, effective masses, and quasiparticle residues as functions of the electron-phonon coupling constant λ for two values of regularization parameters: $\epsilon = 0.2$ (black dashed curves with open circles) and $\epsilon = 0.05$ (red dashed curves with open squares). Error bars are shown in all plots; for energy values they are orders of magnitude smaller than symbol sizes.

In the $(n-1)$ update, called with probability p_-, the last hopping event (if there is one, otherwise the update is rejected) is simply erased from the configuration. The acceptance ratio for the complementary pair of the $(n \pm 1)$ updates equals

$$R = \frac{p_-}{p_+}\frac{W_{n+1}}{W_n}\frac{2(\tau-\tau_n)t(y,z)}{P(y,z)}. \tag{9}$$

Results. Full quantum mechanical solution of the problem confirms the overall picture established on the basis of the energy landscape (5) and finds that the dispersion minimum remains at zero momentum when the quasiparticle residue Z collapses to near zero, the effective mass m_* undergoes an explosive enhancement, and the ground-state energy E exceeds the bare particle half-bandwidth. This behavior, typical for transition to the nearly localized state, is illustrated in Fig. 5 showing E, m_*, and Z as functions of the coupling constant $\lambda = 2g^2t/\Omega$ for two characteristic values of ϵ. (We extract E, m_*, and Z from the Green's function; all details can be found in Refs. [9,15].)

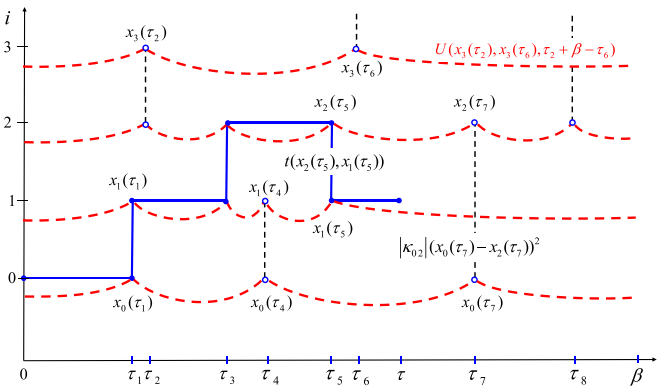

FIG. 6. Typical x-representation diagram for the Green's function $\mathcal{G}(\tau, r)$ for the dispersive-phonon counterpart of the model (2). The particle worldline and the phonon propagators in the x representation have the same meaning as in Fig. 4. The new elements are the vertical dashed lines representing the attractive interaction between auxiliary local modes (cf. Ref. [18]). Note also that now the diagram is extensive: It occupies a macroscopic space-time volume.

Conclusions and outlook. We show that unusual properties of linearized PSSH polarons are absent in a model with sign-definite t_{ij}, thereby emphasizing the importance of nonlinear terms at strong coupling in real materials. In this respect, special attention should be paid to the microscopic physics behind sign-alternating phonon modulated hopping, such as, e.g., competition between the tunneling paths in multiorbital systems [14].

Our results are based on the diagrammatic-type MC approach combining the worldline representation for the particle with the x representation for atomic displacements. It applies to a broad class of polaron problems with arbitrary density-displacement and hopping-displacement couplings, provided the latter originate from the sign-definite hopping. A dramatic simplification of the scheme, with the associated efficiency gain, takes place in models with dispersionless phonons.

For dispersive phonons, the most challenging aspect of exact formulation is the necessity of performing an extensive (macroscopic) integration of all atomic coordinates. There exists a computationally efficient scheme with local (in space-time) Monte Carlo updates. We observe that dispersive phonon modes can be always represented as the result of *attractive* interactions between local modes. The standard diagrammatic expansion in powers of the attractive interaction potential in the x representation is then sign positive and allows efficient MC sampling (cf. Refs. [17,18]; and see Fig. 6). The price one pays for having local updates is the extensive character of the configuration space and the necessity of extrapolating to the thermodynamic ($L \to \infty$) and ground-state ($\beta \to \infty$) limits. An explicit decomposition of the phonon potential energy into a fictitious local part and attractive interactions is as follows (note that the spring constants satisfy the relations $\kappa_{ij} = \kappa_{ji}$ and $\kappa_{ii} > 0$):

$$\sum_{ij}\kappa_{ij}x_ix_j = \sum_i \tilde{\kappa}_i x_i^2 - \sum_{i<j}|\kappa_{ij}|[x_i - \mathrm{sgn}(\kappa_{ij})x_j]^2,$$

$$\tilde{\kappa}_i = \kappa_{ii} + \sum_{j\neq i}|\kappa_{ij}|.$$

Acknowledgments. We acknowledge inspiring discussions with A. Millis, D. Reichman, M. Berciu, C. Zhang, and J. Sous. This work was supported by the National Science Foundation under Grant No. DMR-2032077.

[1] S. Barišić, J. Labbé, and J. Friedel, Phys. Rev. Lett. **25**, 919 (1970).
[2] S. Barišić, Phys. Rev. B **5**, 932 (1972); **5**, 941 (1972).
[3] Yu. Kagan and M. I. Klinger, Zh. Eksp. Teor. Fiz. **70**, 255 (1976) [Sov. Phys. JETP **43**, 132 (1976)].
[4] W. P. Su, J. R. Schrieffer, and A. J. Heeger, Phys. Rev. Lett. **42**, 1698 (1979).
[5] D. J. J. Marchand, G. De Filippis, V. Cataudella, M. Berciu, N. Nagaosa, N. V. Prokof'ev, A. S. Mishchenko, and P. C. E. Stamp, Phys. Rev. Lett. **105**, 266605 (2010).
[6] J. Sous, M. Chakraborty, R. V. Krems, and M. Berciu, Phys. Rev. Lett. **121**, 247001 (2018).
[7] B. Xing, W.-T. Chiu, D. Poletti, R. T. Scalettar, and G. Batrouni, Phys. Rev. Lett. **126**, 017601 (2021).
[8] X. Cai, Z.-X. Li, and H. Yao, Phys. Rev. Lett. **127**, 247203 (2021).
[9] C. Zhang, N. V. Prokof'ev, and B. V. Svistunov, Phys. Rev. B **104**, 035143 (2021).
[10] M. R. Carbone, A. J. Millis, D. R. Reichman, and J. Sous, Phys. Rev. B **104**, L140307 (2021).
[11] A. Götz, S. Beyl, M. Hohenadler, and F. F. Assaad, Phys. Rev. B **105**, 085151 (2022).
[12] C. Feng, B. Xing, D. Poletti, R. Scalettar, and G. Batrouni, arXiv:2109.09206.
[13] C. Zhang, N. V. Prokof'ev, and B. V. Svistunov, Phys. Rev. B **105**, L020501 (2022).
[14] C. Zhang, J. Sous, D. R. Reichman, M. Berciu, A. J. Millis, N. V. Prokof'ev, and B. V. Svistunov, arXiv:2203.07380.
[15] N. V. Prokof'ev, B. V. Svistunov, and I. S. Tupitsyn, Zh. Eksp. Teor. Fiz. **114**, 570 (1998) [J. Exp. Theor. Phys. **87**, 310 (1998)].
[16] N. V. Prokof'ev and B. V. Svistunov, Phys. Rev. Lett. **81**, 2514 (1998).
[17] E. Burovski, N. Prokof'ev, B. Svistunov, and M. Troyer, Phys. Rev. Lett. **96**, 160402 (2006); New J. Phys. **8**, 153 (2006).
[18] M. Boninsegni, N. V. Prokof'ev, and B. V. Svistunov, Phys. Rev. E **74**, 036701 (2006).